

## Article

# Wave Resource Assessments: Spatiotemporal Impacts of WEC Size and Wave Spectra on Power Conversion

Gabrielle Dunkle, Shangyan Zou and Bryson Robertson \* 

School of Civil and Construction Engineering, Oregon State University, 1791 SW Campus Way, Corvallis, OR 97333, USA; dunkleg@oregonstate.edu (G.D.); zoush@oregonstate.edu (S.Z.)

\* Correspondence: bryson.robertson@oregonstate.edu

**Abstract:** Wave energy has the potential to power significant portions of economies around the world. Standard International Electrotechnical Commission methods for determining wave energy quantifies the gross wave resource available in the ocean, yet a significant portion of this resource is not usable by specific wave energy converters (WECs). This can provide a misleading assessment of the spatiotemporal opportunities for wave energy in deployment locations. Therefore, there is a need to develop a new technique to assess potential wave power from a device point of view that is generally applicable across WEC sizes. To address this challenge, a novel net power assessment methodology is proposed, which implements Budal's upper bound (which describes the power available to a WEC based on its stroke), the radiation power limit (which describes the maximum radiation-based amount of wave power a WEC can absorb), and total gross incident wave power as absorbable power upper bounds. Spatiotemporal opportunities for WECs were re-evaluated based on this new technique. Numerical simulations were conducted to quantify the net wave resource available for different sized WECs (1, 2, 5, 10) at five different ocean sites in the U.S. based on wave data. The simulation results show the predicted potential wave power through the net power assessment for a 5 m device is 0.8% of the International Electrotechnical Commission assessment results at PacWave, Oregon. For the monthly average power, the results show PacWave has the most energetic wave resource (up to 406 kW in January) and WETS, Hawaii, has the steadiest wave power available (maximum COV of 0.8) among the sites. Regarding the size of the devices, results show that larger devices (e.g., 10 m) have better performance in terms of both magnitude and steadiness of power available at WETS and Los Angeles, California. Finally, the wave power potential of different sized WECs at varying locations was compared at a 3-h resolution. The maximum instantaneous power available for a 1 and 10 m device at PacWave throughout the time period was 47.8 and  $3.52 \times 10^3$  kW, respectively.

**Keywords:** wave energy converters; wave resource assessments; marine renewable energy; net power assessment (NPA)



**Citation:** Dunkle, G.; Zou, S.; Robertson, B. Wave Resource Assessments: Spatiotemporal Impacts of WEC Size and Wave Spectra on Power Conversion. *Energies* **2022**, *15*, 1109. <https://doi.org/10.3390/en15031109>

Academic Editor: Eugen Rusu

Received: 22 December 2021

Accepted: 28 January 2022

Published: 2 February 2022

**Publisher's Note:** MDPI stays neutral with regard to jurisdictional claims in published maps and institutional affiliations.



**Copyright:** © 2022 by the authors. Licensee MDPI, Basel, Switzerland. This article is an open access article distributed under the terms and conditions of the Creative Commons Attribution (CC BY) license (<https://creativecommons.org/licenses/by/4.0/>).

## 1. Introduction

Opportunities for renewable energy are becoming increasingly abundant given the global need for decreased dependence on fossil fuels. Inclusion of ocean renewable energy sources could be a valuable additional energy source for global decarbonization. Wave energy holds particular interest due to its consistency, magnitude, and the great amount of power per area [1]. Neil and Hashemi [2] predict that the use of ocean renewables will continue to consistently increase and are projected to contribute 748 gigawatts (GW) to the global energy supply by 2050.

As with all renewable energy technologies, estimation of technology power production and energy conversion is dependent on the gross resource available and the efficiency of the technology to harness and convert the gross resource into usable power. Traditionally, wave energy technology and project developers have focused on developing multi-megawatt

(MW) projects for terrestrial utility-scale applications. Recently, using wave power to support small non-grid applications (e.g., power ocean observation buoys [3], deep sea autonomous underwater vehicle (AUV) charging stations [4], or other Blue Economy) has attracted significant research attention (kW-level). In fact, recent research supports the motivation for increased small WEC utilization, as some widely accepted WEC designs may lack scalability [5].

Regardless of the sizes of the WECs, typically, the wave energy converter (WEC) developers follow the standardized guidelines for wave resource assessments published by the International Electrotechnical Commission (IEC) to find the gross amount of wave power available in the sea and, subsequently, create technology [6]. However, the IEC standards evaluate the gross wave power available based purely on general wave characteristics, a great portion of which is not directly absorbable by WECs (even for utility-scale WECs). Therefore, there is a clear need to develop a new generic WEC net power assessment technique that provides a more conservative/accurate estimation of the available wave power and accounts for the dimensions of the device. In this paper, a novel WEC net power assessment (NPA) approach is developed and is applicable to generic WECs sizes by applying the theoretical and physical upper bounds.

Generally, the theoretical upper bounds limiting WEC power absorption are based on the device's radiated wave pattern ( $P_a$ ) [7], the device's characteristic width ( $D$ ), and the volume stroke ( $P_b$ ) [8]. Budal and Falnes [8] derived methods for determining the wave power absorbable by a heaving WEC using theoretical upper bounds to calculate maximum absorption by considering the volume stroke. In this theory, it is assumed that the maximum absorbable power is limited by the excitation power, which depends on the WEC's size, stroke, and the surrounding wave frequency [9]. This concept, dubbed Budal's upper bound, was subsequently established and has been utilized in research since 1980.

Budal and Falnes continued to refine limits for WEC power capture [8,10]. During the early 2000s, Falnes became the first to integrate the radiation power limit and Budal's upper bound for determining absorbable power to devices [11,12]. This path of research was focused on small WECs that could extract relatively less power than MW-scale devices [13]. From here, others began re-investigating WEC control methods for implementation to achieve the maximum power described by Budal's upper bound and the radiation power limit [14]. Research thus far used unit analytical values to assess maximum power absorption for given WEC sizes.

In terms of the status quo, Budal's upper bound has been used in tandem with the WEC radiation power limit to determine absorbable wave power. The WEC radiation power limit depends on the wave patterns the WEC itself develops [7]. Incoming incident waves interact with a body, forcing it to oscillate in the water column. A heaving device will act as a source radiation point, with circular waves diffusing from its body. How well the WEC can absorb incoming wave power is contingent upon the interaction between the device's outgoing radiated wave and the incident wave.

More recently, Beatty et al. [15] examined theoretical power absorption for two self-reacting point absorber (SRPA) WECs, each comprised of two bodies and power take-off controls. Beatty et al. extended Budal's upper bound for this type of device and used the radiation power limit for heaving devices to determine absorbable wave power [15]. The team applied the power limits to experimental wave data obtained from wave tank experiments. Results showed that experimental absorption for the SRPAs was much lower than theoretical absorption levels, between 40 and 85% less [15].

However, the radiation power limit and Budal's upper bound have yet to be applied to non-analytical, non-experimental cases. Specifically, Budal's upper bound is rarely implemented, despite being frequently referenced in research, and the upper limit has seen no application on real-world wave spectra. Understanding the implications of applying these theoretical to real wave spectra is paramount to understanding their long-term utility to the WEC industry.

This study aims to provide a spatiotemporal analysis of WEC-size agnostic methods for determining net power available to devices. Using the radiation power limit and Budal's upper bound, traditional wave resource assessment-calculated gross wave power is filtered to find absorbable wave power in what is called a WEC net power assessment (NPA). As wave energy expands into new opportunities and sectors, methods for quantifying the potential absorbable power are necessary. This paper is structured as follows: Section 2 introduces standard IEC wave resource assessments and the novel WEC NPA methodologies. Section 3 provides an overview of the five study locations around the United States and the scenarios used to help elucidate the impact of this research. Section 4 provides an overview of the results of this new methodology, while Section 5 discusses the implications and assumptions inherent to this research. Finally, Section 6 provides a conclusion of the research findings.

## 2. Materials and Methods

The traditional method to quantify the resource for wave energy follows guidelines developed by the International Electrotechnical Commission (IEC). A consensus-based organization, the IEC convenes experts from around the world to develop technical specifications and standards to ensure safety and efficiency in a wide variety of sectors. However, as previously described, the current IEC specifications are not suitable to the expanding scope of applications for the wave energy industry, and novel methods for quantifying the net power available for absorption and conversion across a wide variety of WEC scales and sizes are necessary.

### 2.1. Traditional Wave Resource Assessment Methods

An internationally recognized methodology for gross wave energy resource assessments converged under a set of guidelines published by the IEC in 2015 [16]. The technical specification (TS) 62600-101 aims to standardize the methodology and output parameters necessary for a robust wave resource assessment. Ocean wave parameters necessary to characterize the wave resource include significant wave height ( $H_{m0}$ ), energy period ( $T_e$ ), omni-directional wave power ( $J$ ), the directionally resolved wave power and its direction ( $J_\theta$  and  $\theta_{j\theta_{max}}$ ), directionality coefficient ( $d$ ), and spectral width ( $\epsilon_0$ ).

These values are calculated from the directional wave spectrum ( $S_{ij}$ ), which may be obtained via numerical modeling or physically observed measurements [16]. For the simplest of assessments (Class 1), significant wave height, energy period, and omni-directional wave power are required. To calculate omni-directional parameters, the 1D frequency spectrum must first be calculated via:

$$S_i = \sum_j S_{ij} \Delta\theta_j \quad (1)$$

where  $S_{ij}$  is the variance density in the  $i$ th frequency and  $j$ th directional bin and  $\Delta\theta_j$  is the directional bin spacing. Spectral moments of the  $n$ th order,  $m_n$ , are calculated from frequency variance density by:

$$m_n = \sum_i f_i^n S_i \Delta f_i \quad (2)$$

The characteristic wave height,  $H_{m0}$  is calculated using the zeroth spectral moment:

$$H_{m0} = 4\sqrt{m_0} \quad (3)$$

The preferred characteristic wave period for wave resource assessments is the energy period:

$$T_e = \frac{m_{-1}}{m_0} \quad (4)$$

Omni-directional wave power, or simply wave power,  $J$ , is the time-averaged energy flux through a vertical cross section of unit diameter that extends from the seafloor to the surface, calculated by:

$$J = \rho g \sum_{i,j} c_{g,i} S_{ij} \Delta f_i \Delta \theta_j \quad (5)$$

where  $c_{g,i}$  is the group celerity,  $\rho$  is the water density, and  $g$  is the gravitational constant. These equations may be found in IEC TS 62600-101 [16].

At a minimum, the monthly averages over a 10-year time period, along with a  $H_{m0} - T_e$  histogram, are required for a Class 1 assessment [16]. Additionally, any influential environmental parameters must be considered but only for higher resolution assessments. Class 2 and Class 3 IEC assessments require increased spatial (20–500 and <25 km, respectively) and temporal (3 and 1 h, respectively) resolution of wave data and should be based directly on measured wave spectra or a measure–correlate–predict method [16]. Interested readers can find the full derivation of the guidelines in the IEC TS 62600-101 [16].

## 2.2. WEC Net Power Assessment (NPA)

The WEC net power assessment (NPA) is a novel methodology for determining the maximum net, or absorbable, wave power available for extraction by a given WEC device. The radiation power limit ( $P_a$ ) and Budal's upper bound ( $P_b$ ) are used to filter the gross power ( $P_{gross}$ ) found from the traditional IEC wave resource assessment to find the net absorbable power for each WEC device.

The radiation power limit ( $P_a$ ) is determined by the radiation patterns of the waves generated by the WEC itself, as explained previously [14]. This power limit is the product of the incident wave power and the maximum absorption width of a heaving WEC device, as shown in Equation (6):

$$P_a = \frac{\rho \left(\frac{\pi}{8}\right)^3}{128} H^2 T^3 \quad (6)$$

where  $H$  is wave height and  $T$  is wave period for a regular sinusoidal wave for an axisymmetric WEC [17]. The derivation of the radiation power limit presented in Equation (6) requires the WEC to only move in heave, i.e., act as a source [11]. This limit also assumes the waves occur in deepwater and estimates power in Watts (W).

Budal's upper bound ( $P_b$ ) is an upper bound for WEC power absorption based on the assumption that the device is small and does not disturb the surrounding wave field. As an upper bound, this eliminates the total power's dependence on the radiated, hydrostatic, frictional, PTO, and mooring forces [8]. Therefore, the power absorbable by the device is equal to the excitation power of the waves onto the WEC ( $P_e$ ). According to small body theory, excitation power and, therefore, Budal's upper bound, are equal to:

$$P_b = \frac{1}{2} \rho g S_w A \omega s_{max} \quad (7)$$

where  $S_w$  is the water plane area of the device at the surface,  $A$  is the wave amplitude,  $\omega$  is wave frequency, and  $s_{max}$  is the maximum stroke of the WEC [8,11,14,15]. The device's size and stroke along with the incident wave amplitude are the driving factors behind Budal's upper bound.

Both the radiation power limit and Budal's upper bound require a regular wave height ( $H$  for  $P_a$ ,  $\frac{1}{2}H = A$  for  $P_b$ ). This value can be found by relating the spectral density and its specific wave heights using Equation (8):

$$S(w) = \frac{A^2}{2\Delta f} \quad (8)$$

where  $S(w)$  is the spectral density,  $A$  is the wave amplitude, and  $\Delta f$  is the frequency spacing of the spectrum [18].

Gross wave power is found by multiplying the omnidirectional wave power  $J$  found from the IEC assessment (Equation (5)) by the characteristic width of the device, i.e., the width of the device interacting with the incoming waves,  $D$ :

$$P_{gross} = J \times D \quad (9)$$

Net power can be found by essentially “filtering” the gross power: the radiation power limit and Budal’s upper bound are calculated, and any gross power greater than the two limits is considered nonexistent. This resulting net power represents the theoretical maximum absorbable power by the WEC of interest.

Figure 1 shows the Budal diagram of a 5 m WEC with a unit wave height and wave period varying from 0 to 30 s. The red line is the radiation power limit ( $P_a$ ), which increases exponentially as the wave period increases. The region underneath the two limits is theoretically absorbable by the WEC. However, following this theoretical method results in WEC production that can exceed the gross wave power available in the ocean. This is shown in Figure 2, where the green line ( $P_{gross}$ ) indicates the gross power available in the waves. Instead of limiting the gross power, the radiation power limit and Budal’s upper bound actually over-predict the realistic net WEC power absorption potential.

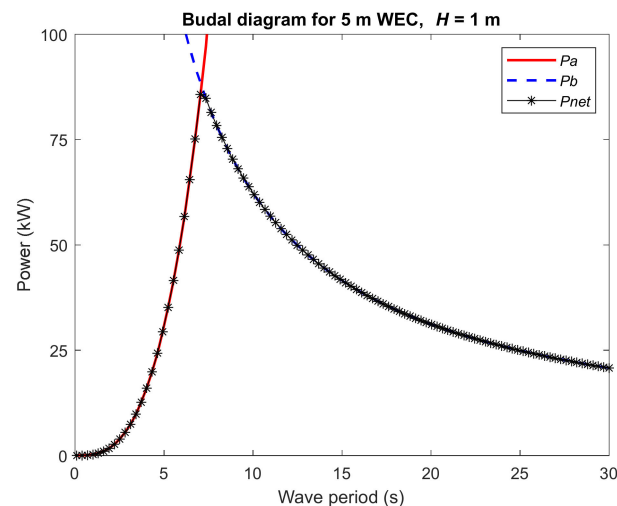


**Figure 1.** Budal diagram for a 5 m WEC. The black star line corresponds to the net power extractable by the device.

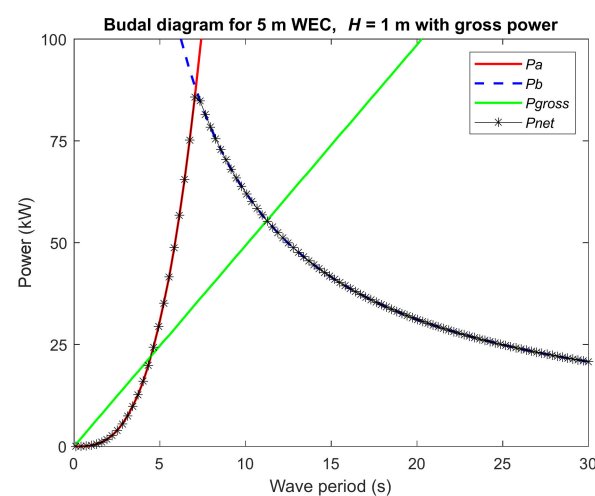


**Figure 2.** Budal diagram for a 5 m WEC, with the addition of gross wave power (green).

As discussed in the Introduction, these two power limits have previously been used to analytically quantify the theoretical amount of power absorbable by a limited range

of WECs [11,19,20]. Beatty et al. [15] applied these limits to a self-reacting point absorber (SRPA) WEC. Beatty et al. imposed practical constraints to the radiation power limit and Budal's upper bound by limiting the maximum vertical stroke of their devices, or  $s_{max}$  in Equation (7). Instead of allowing the SRPAs to oscillate freely in the water column, their vertical stroke was constrained in order to prevent excessive PTO stroke lengths from occurring [15]. To validate the NPA methodology against published experimental results, the results from Beatty et al. are plotted against the radiation power limit and Budal's upper bound for the Reference Model 3 (RM3) two-body point absorber [21] WEC. The results are shown in Figure 3.

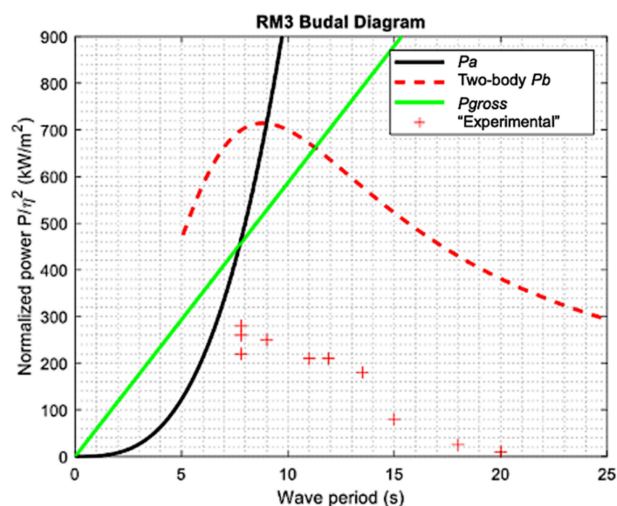


**Figure 3.** Recreation of Beatty et al.'s research using RM3 WEC data. The black solid line is the radiation power limit, the dashed red line is Budal's upper bound for [15] body A, the red crosses are experimental data points that were found by Beatty et al. [15], and the solid green line is the gross incident wave power that interacts with the device. Here, the y-axis describes the wave power normalized by wave amplitude squared ( $\eta^2$ ).

The black solid line in Figure 3 shows the radiation power limit, while the red dashed line shows Budal's upper bound. In addition to the radiation power limit and Budal's upper bound used by Beatty et al. [15], this present study factored in gross wave power as a limitation. Realistically, no wave power greater than gross power exists in the ocean; it is essential to include gross power as an upper limit for absorbable wave power.

Real waves in the ocean are not perfect regular sinusoidal waves, as assumed in all the presented work thus far. Figure 4 shows the wave spectrum for one hour at PacWave. PacWave is an open-ocean test site for WECs, currently in development off the Oregon coast, USA. As shown, ocean sea states feature a wide spectrum of variable wave heights and periods. Completing an NPA requires applying the power limits to a spectrum such as that seen in the results in Figure 4. As shown in Figure 5, net power is limited by the gross power available at middle-range wave periods, while long wave periods are constrained by Budal's upper bound and gross power, and short wave periods are restricted by the radiation power limit.

When applied to a wave spectrum, the general shape of the power limit curves takes on a more realistic form to mimic the wave spectrum of interest. However, the general behavior of the limits remains the same as regular wave theory.

Metrics used to analyze the NPA results included mean annual average energy production (MAEP), average power, coefficient of variation (COV), and percent reduction. MAEP was calculated via Equation (10):

$$MAEP = \Sigma J \times D \times \text{Average Annual Occurrence} \quad (10)$$

where  $J$  is the omnidirectional wave power and  $D$  is device diameter. This parameter is useful for determining the bulk wave capture of a device size and site.

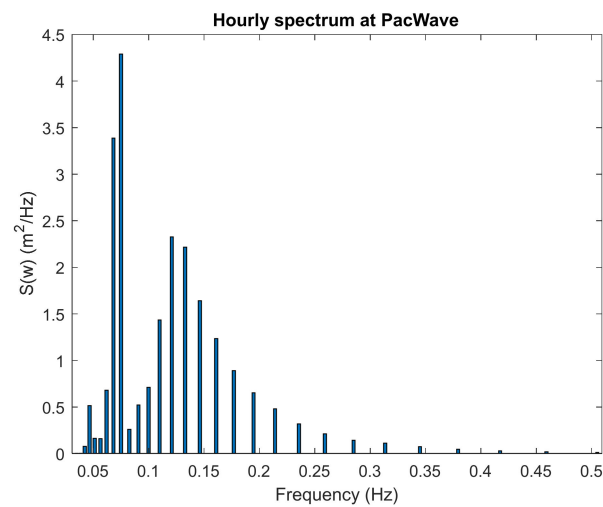


**Figure 4.** Wave spectrum for one hour at PacWave.

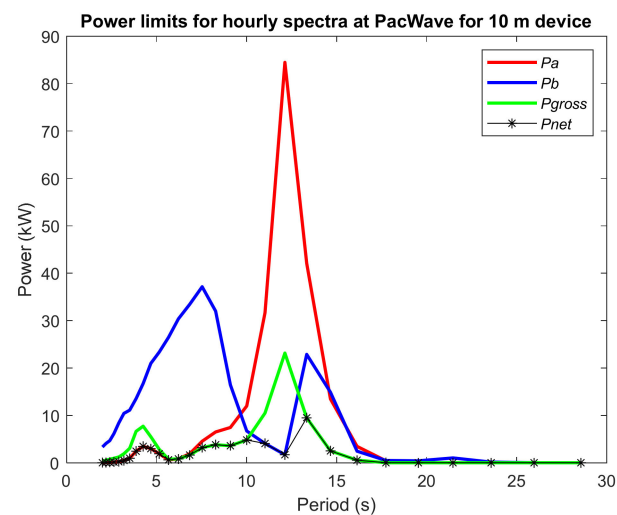


**Figure 5.** Power limit behavior and resulting net power for the hourly spectrum at PacWave for a 10 m WEC.

The COV is a measure describing the temporal variability, or overall steadiness, of the wave resource at a given site. It is found via Equation (11):

$$COV = \frac{\sigma}{\mu} \quad (11)$$

where  $\sigma$  is the standard deviation of the wave power and  $\mu$  is the mean wave power [22]. A higher value of COV indicates a less steady resource, while values under 1 indicate a less temporally variable wave power resource at a site.

Percent reduction is the ratio in percentage of a reduced quantity to its initial value. Percent reduction can be calculated via Equation (12), and in this study, the metric was used to calculate the difference between the IEC-calculated gross wave power and the absorbable net power calculated via the NPA:

$$Percent\ reduction = \frac{P_{gross} - P_{net}}{P_{gross}} \times 100\% \quad (12)$$

### 3. Case study WEC, Assessment Locations, and Study Scenarios

To understand the spatiotemporal interactions between gross wave resources, sea state conditions, WEC size, and the net power production opportunity, a single WEC concept, five (5) assessment locations (outlined in Table 1), and a variety of study scenarios were developed.

**Table 1.** Locations for wave resource and WEC net power assessments.

Location	Lat, Lon (Degrees)	Depth (m)
PacWave, OR, USA	44.557, −124.229	68
Los Angeles, CA, USA	33.854, −118.633	350
WETS, Oahu, HI, USA	21.466, −157.751	34
Cape Cod, MA, USA	41.140, −70.690	38
Miami, FL, USA	25.460, −80.030	318

A simple spherical WEC was chosen for analysis in this study, a general description of which is shown in Figure 6. This WEC is a heaving axisymmetric device with generic reactive control and design for all subsystems (e.g., PTO, energy storage, mooring); in the context of this research, a specific design of a subsystem is out of scope. The heaving degree of motion was chosen, as the original Budal's upper bound was derived for these types of devices. Four characteristic device widths (in this case, diameters) were investigated. Heaving spherical WECs of 1, 2, 5, and 10 m were chosen for analysis to capture a wide range of device sizes.

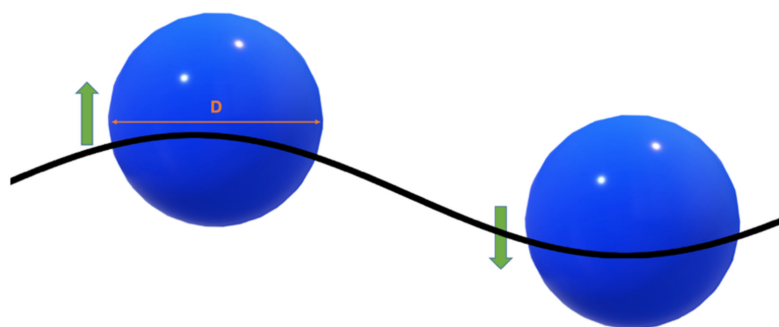


**Figure 6.** Basic schematic of the heaving spherical WEC used in this study. The device captures energy by oscillating vertically (heaving) in the water column as incident waves interact with it. The heaving induces movement in a turbine, which converts the motion to usable power.

This study completed both a traditional IEC wave resource assessment (according to IEC TS 62600-101 [16]) and a WEC NPA for five different study locations outlined in Table 1: PacWave, Oregon; Los Angeles, California; WETS, Oahu, Hawaii; Cape Cod, Massachusetts; and Miami, Florida. PacWave, Oregon, was chosen since it is an existing wave energy test site aimed at testing utility-scale ocean resources [6]. Down the West Coast from PacWave is Los Angeles, California, a site chosen since it is close to a major city and has a documented small yet stable wave resource [22]. Off the eastern coast of Oahu, Hawaii, is the Wave Energy Test Site (WETS), chosen for analysis due to its existing WEC testing infrastructure and stable wave resource [23].

On the East Coast of the United States, Cape Cod, Massachusetts, was chosen as it is near major population hubs, has a medium-sized wave resource, and is close in proximity to the proposed Vineyard Wind Farm location, opening potential opportunities for tandem wave–wind converter devices [22]. Finally, Miami, Florida, was chosen for analysis since it has been classified as unusable for present state-of-the-art WEC devices [24]; this study aims to determine if small WECs would be suitable to capture wave energy off Florida's southern coast. Figure 7 shows the study locations and the gross wave energy transport, as developed and calculated by Cornett [22].



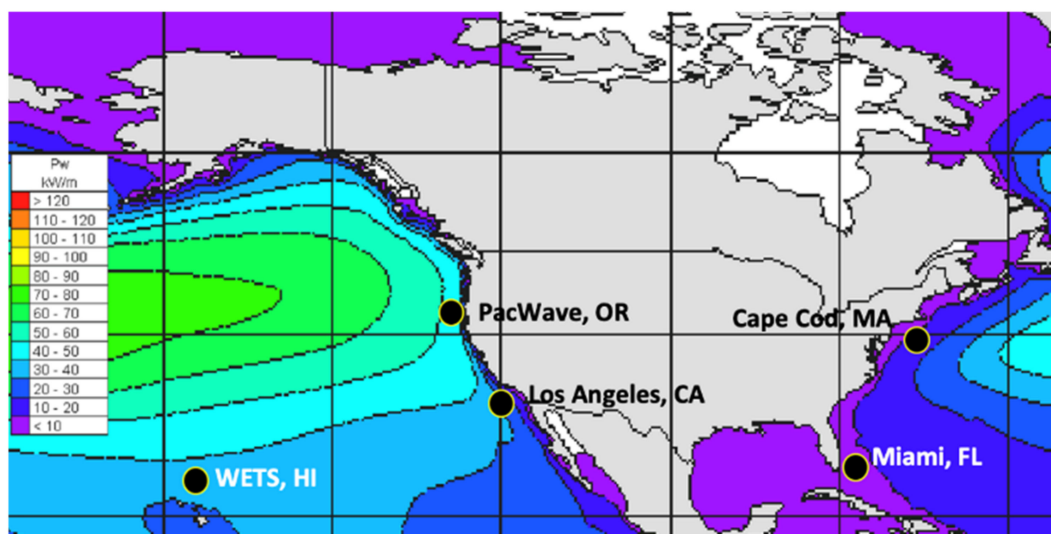


**Figure 7.** Study locations (black dots with yellow outline) shown on a base map of gross wave power (Cornett, 2008).

Spectral wave data were obtained from Pacific Northwest National Laboratories (PNNL) and from the Sandia National Laboratory. The PNNL hindcast was focused on the West Coast of the U.S. and used a nested-grid WaveWatch III model (WWIII) on both global and regional scales [25]. Their WWIII model was paired with a high-resolution, unstructured-grid Simulating Waves Nearshore (SWAN) model for near-shore regions [25]. The Sandia National Lab hindcast was focused on the East Coast of the U.S. and used a high-resolution SWAN model, forced by the Climate Forecast System Reanalysis (CFSR) winds and WWIII wave boundary conditions [26]. Data from both models between 2000 and 2010 (11 years) were analyzed to account for potential seasonality for both the IEC and WEC net power assessments. Hourly wave spectra encompassing 29 frequencies and 36 directions were transformed to hourly 1-D frequency spectra via MATLAB computing software.

Two assessment scenarios were evaluated: the baseline scenario, based on the methods from existing literature using the radiation power limit and Budal’s upper bound, and a novel expanded scenario. In the expanded scenario, gross power was used to filter absorbable power along with the radiated power limit and Budal’s upper bound. The details of the two scenarios analyzed in this study are shown in Table 2.

**Table 2.** Description of scenarios analyzed in this study.

	Baseline Scenario	Expanded Scenario
Filters	$P_a, P_b$	$P_a, P_b, P_{gross}$
Maximum stroke	$s_{max} = \begin{cases} 25\% \text{ of } D & H > 0.25D \\ H & H < 0.25D \end{cases}$	$s_{max} = \begin{cases} 25\% \text{ of } D & H > 0.25D \\ A & H < 0.25D \end{cases}$

#### 4. Results

In this section, the numerical investigation of the novel proposed wave power assessment technique is discussed across different sizes and locations. The computing software MATLAB was used to investigate 11-years’ worth of wave spectra at each of the sites, parsing analyses into yearly, monthly, and hourly quantities. Temporally variable values of omnidirectional wave power were the primary subjects of the WEC net power assessments across the five ocean test sites.

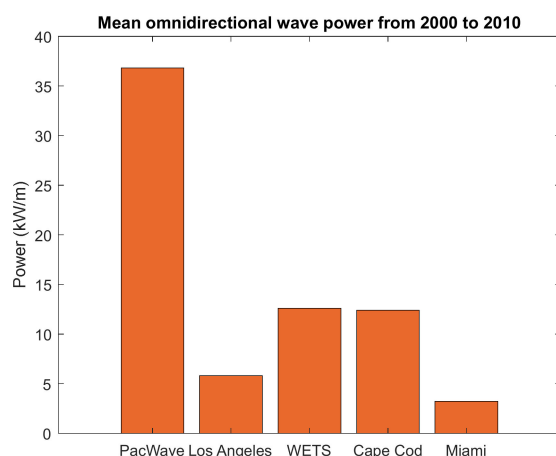
##### 4.1. IEC Assessment

The IEC-calculated significant wave height  $H_{m0}$ , energy period  $T_e$ , and omnidirectional wave power  $J$  are presented in Table 3.

**Table 3.** Mean and maximum values for significant wave height, energy period, and omnidirectional wave power at each study location from 2000 to 2010.

Location	Max $H_{m0}$	Mean $H_{m0}$	Max $T_e$	Mean $T_e$	Max $J$	Mean $J$
PacWave, OR, USA	9.70 m	2.30 m	19.80 s	9.70 s	719 kW	36.8 kW
Los Angeles, CA, USA	4.03 m	1.07 m	16.5 s	9.38 s	80.3 kW	5.81 kW
WETS, Oahu, HI, USA	4.46 m	1.66 m	15.4 s	7.59 s	145 kW	12.6 kW
Cape Cod, MA, USA	7.44 m	0.857 m	12.9 s	5.49 s	256 kW	3.24 kW
Miami, FL, USA	7.33 m	1.55 m	16.6 s	6.78 s	344 kW	12.4 kW

PacWave, Oregon, is one of the most energetic locations in the world, with gross annual wave power ranging between 40 and 50 kW/m on average according to Cornett [22]. The IEC assessment reinforced this, finding that the average omnidirectional wave power over the course of 2000–2010 was 36.8 kW/m, as seen in Figure 8. WETS, Hawaii, has the next highest amount of wave resource with 12.6 kW/m per year on average from 2000 to 2010, followed by Los Angeles, Cape Cod, and Miami, both according to Cornett [22] and this assessment (Figure 8).

**Figure 8.** Mean yearly omnidirectional wave power at all study sites from 2000 to 2010.

Miami possesses the lowest omnidirectional wave power over the course of the study period yet has the second-largest significant wave height. This is due to the intense hurricane and tropical storm seasons that Florida experiences each year [27]. Cape Cod, also on the Atlantic Coast, ranks higher than WETS with average significant wave height, yet has slightly less average omnidirectional wave power. Again, this is due to the yearly hurricane season that produces large waves. For readers interested in the IEC wave resource assessment process and results for each location in greater detail, please see Dunkle (2021) [28].

#### 4.2. WEC Net Power Assessment (NPA)

Instead of using the IEC standards to assess the available wave power purely from a wave point of view, this research proposes to conduct wave power potential assessment directly from a device point of view (the WEC NPA methods). As presented in Section 3, there are two methods explored in this study, the baseline and expanded scenarios, shown in Figures 9 and 10, respectively. The wave conditions applied in these two figures have a unit wave height of 1 m and wave periods varying from 0.1 to 30 s in order to determine the frequency dependence of the power limits against a realistic (but slightly expanded) set of wave periods. Based on the expression of the radiation power limit presented in Section 2.2, the radiation power limit does not vary based on different WEC sizes (which is consistent with the observations from Figure 9). In contrast, Budal's limit is dependent on WEC size and becomes larger as devices increase in size. By further comparing with the gross wave power (the green line in Figure 10), it is clearly visible that there is a significant portion of

the radiation power limit ( $P_a$ ) and Budal's upper bound ( $P_b$ ) that is actually higher than the gross wave power. This phenomenon is not realistic since gross wave power is considered as all of the power in the ocean waves. In addition, the maximum power absorbable by the 10 m device decreases by 100 kW for the 1 m wave height when using the expanded scenario methods compared to the baseline. The 5 m net power decreases by 35 kW for the 1 m wave height, while the 2 and 1 m devices do not change. This occurs because 25% of the radius of the 1 and 2 m devices is equal or less than the wave height of 1 m; therefore, the maximum stroke for both the expanded and baseline scenarios is restricted to the device diameter. Ultimately, it is more practical to apply the expanded scenario rather than the baseline methods since it does not exceed the gross wave power and provides a more conservative estimate in comparison.

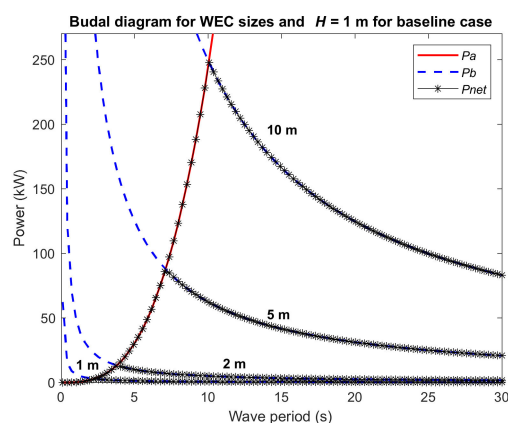


**Figure 9.** Budal diagram showing Budal's upper bound for different WEC sizes compared to the radiation power limit for the baseline scenario methods. Net power absorbable is outlined in a black star line. Each net power curve is labeled according to its corresponding WEC characteristic length (i.e., body diameter). The lowest curve is for the 1 m device, followed increasingly by the 2, 5, and 10 m device net power curves.

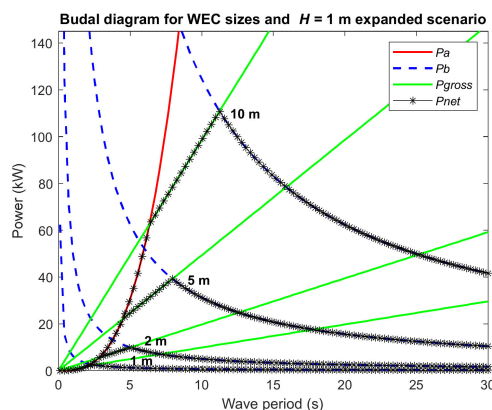


**Figure 10.** Budal diagram showing Budal's upper bound for different WEC sizes compared to the radiation power limit and gross wave power for the expanded scenario methods. Net power is outlined in a black star line. Each net power curve is labeled according to its corresponding WEC characteristic length (i.e., body diameter). The lowest curve is for the 1 m device, followed increasingly by the 2, 5, and 10 m device net power curves.

Representative sea states from Pierson–Moskowitz (PM) spectra were chosen to determine how the two scenarios compared when applied to quasi-realistic wave spectra. The two PM spectra used for analysis are shown in Figure 11a,b, which have a significant wave height of 1 m and peak periods of 8 and 12 s, respectively.

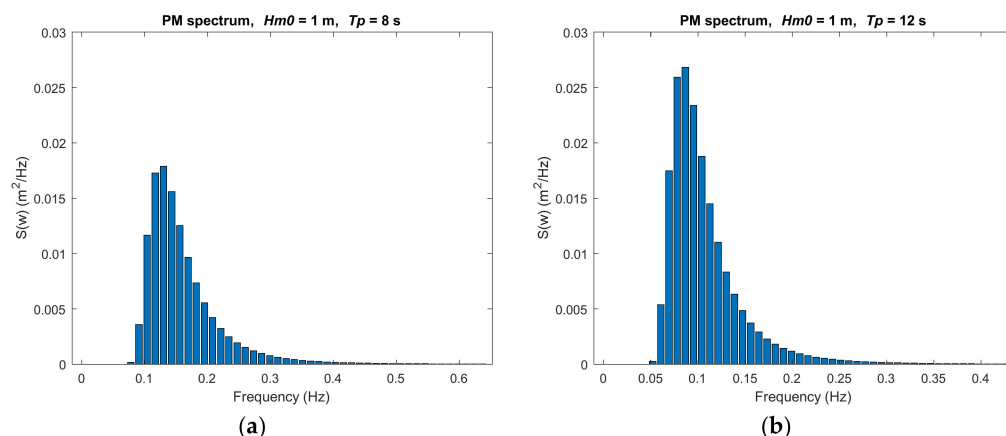


**Figure 11.** PM spectrum with significant wave height of 1 m and peak period of (a) 8 s and (b) 12 s.

As shown in Figures 12 and 13, the 1 and 10 m device sizes were selected to represent the results of the NPA methods imposed on the PM spectra (with a significant wave height of 1 m and a peak period of 8 s). Both the baseline and expanded scenarios were examined, and the net power outputs were plotted. For both WEC sizes, the expanded scenario method yields less absorbable wave power than the baseline scenario method. This was expected due to the more restrictive (constrained by a more conservative Budal's upper bound) and realistic constraints (bounded by the gross wave power) of the expanded scenario. It is possible to tell that gross power limits the total net power by observing the baseline net power values, and how much greater the values are than the gross power at certain points (e.g., between wave period of 1–4.5 s for the 1 m device and between 5 and 13 s for the 10 m device).

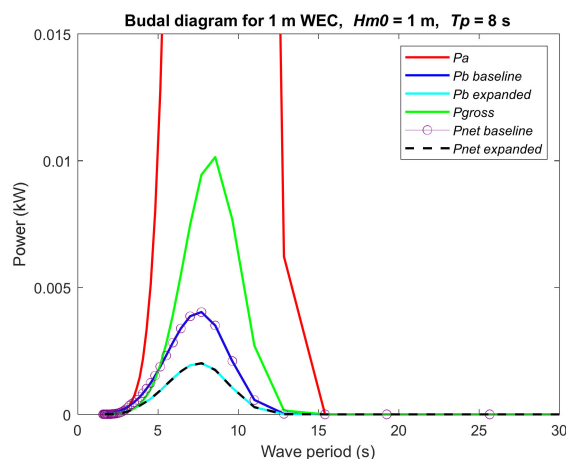


**Figure 12.** Radiation power limit, Budal's upper bound, gross power, and net power for 1 m WECs for a PM spectrum of 1 m significant wave height and 8 s peak period. Both the baseline and expanded case results are shown.

For the 1 m WEC at mid-range periods, it was determined that Budal's upper bound is the limiting restriction on net wave power since the net power values are smaller than both the radiation power limit and the gross power. At very low wave periods (i.e.,  $T < 1$  s), the radiation power limit is the restricting factor, while gross power limits net wave power to a 2–3.5 s wave period for the expanded case. Budal's upper bound for the expanded scenario limits net power absorption to a 3.5–15 s wave period for the 1 m device.

The 10 m device's net absorbable power for this PM spectrum has a wider variety of limitations. For wave periods greater than 6.4 s through those equal to 15 s, gross power limits net power for the expanded scenario until all the limits converge to similar values after 15 s. The baseline scenario's net absorbable power is limited primarily by the radiation power limit throughout all wave periods, and when compared to the expanded scenario

net power, the difference in methodology is stark. Maximum net power for the baseline scenario is about twice as large as the expanded scenario, demonstrating just how much of an implication including gross power is.

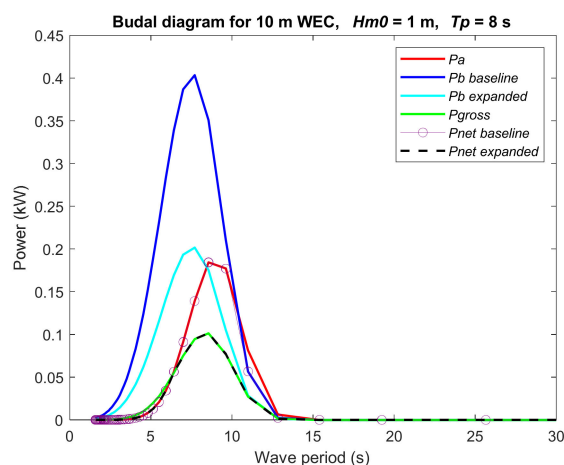


**Figure 13.** Radiation power limit, Budal's upper bound, gross power, and net power for 10 m WECs for a PM spectrum of 1 m significant wave height and 8 s peak period. Both the baseline and expanded case results are shown.

Similar results are shown for the PM spectrum corresponding to a significant wave height of 1 m and peak period of 12 s, in Figure 14. The 1 m device is mostly limited by Budal's upper bound for the baseline and expanded scenario methods. The 10 m device is limited by the gross power between 5 and 12 s for the expanded scenario. In Figure 15, Budal's upper bound limits the baseline net power from 9 s through the rest of the wave periods.

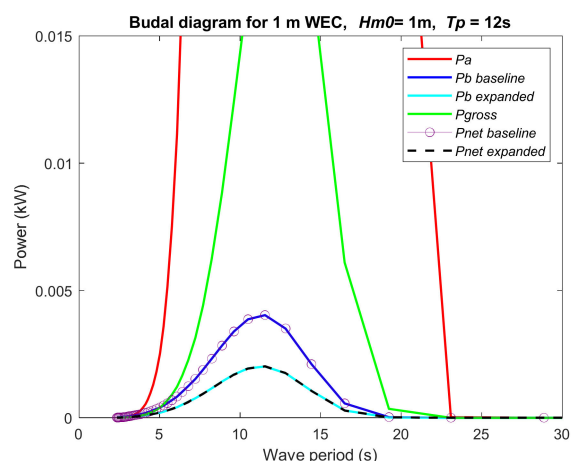


**Figure 14.** Radiation power limit, Budal's upper bound, gross power, and net power for 1 m WECs for a PM spectrum of 1 m significant wave height and 12 s peak period. Both the baseline and expanded case results are shown.

The purpose of this analysis was to determine the effects of baseline and expanded scenario methods for calculating Budal's upper bound and how these apply to quasi-realistic wave spectra. As indicated in the figures, the gross wave power limits the net absorbable power for the WECs (especially as the device size increases). Therefore, it is essential to include this metric in the NPA since no wave power exists beyond the gross wave power. As part of the expanded scenario methods, net power is calculated by the restricted Budal's upper bound, radiation power limit, and gross power. The expanded scenario methods are therefore considered the NPA methods and are evaluated further in the following results.

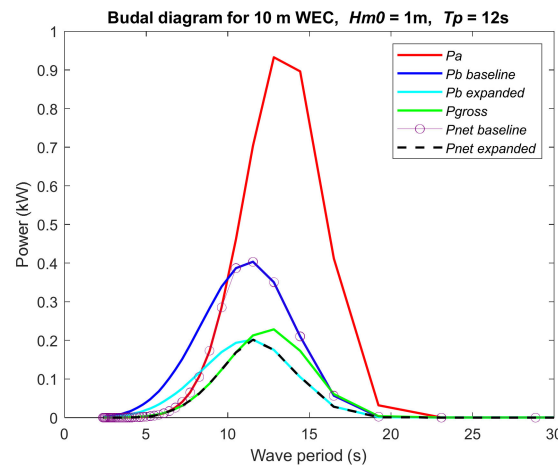


**Figure 15.** Radiation power limit, Budal’s upper bound, gross power, and net power for 10 m WECs for a PM spectrum of 1 m significant wave height and 12 s peak period. Both the baseline and expanded case results are shown.

4.2.1. Mean Annual Average Energy Production

The mean annual average energy production (MAEP) is evaluated based on the proposed power potential assessment for different ocean sites. The results for the 5 m WEC were chosen for representation. As shown in Figure 16, the MAEP for the sites is greatest at PacWave, followed by WETS, Cape Cod, Los Angeles, and Miami. This finding is supported by those of the IEC assessment conducted as part of this study. Figure 16 also shows that certain sites have comparable MAEP. For instance, WETS has an MAEP of 1047 kWh for the 5 m device, while Cape Cod has 896 kWh. Consistently, the IEC-calculated wave power was much larger than the expanded case—this is to be expected since the IEC provides a measure of total gross wave power, while the expanded methods yield a measure of absorbable wave power. This is expressed by comparing Figure 16a,b, and reinforced in Tables 4 and 5 in the following analysis, where instantaneous power and the percent reductions between the IEC and expanded case are shown.

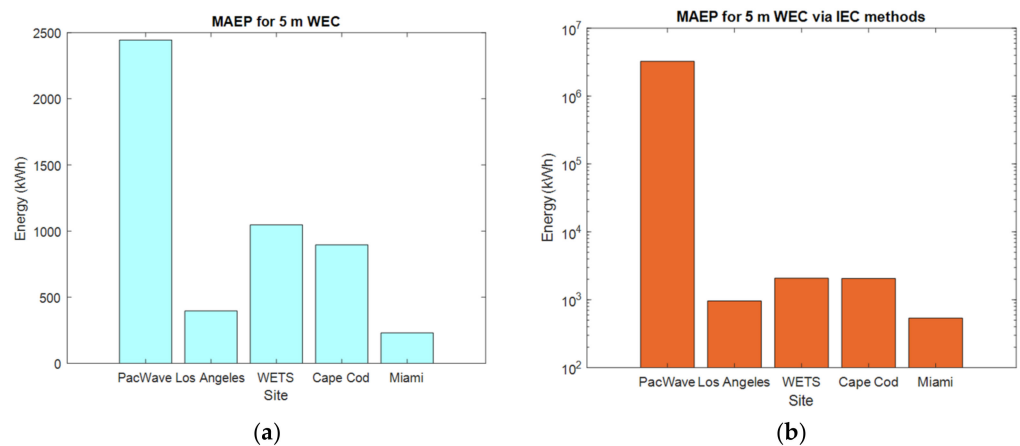


**Figure 16.** MAEP for the 5 m WEC at each study site for the (a) NPA assessment and (b) the IEC assessment methods.

As Figure 16 shows, the MAEP for the 5 m WEC differs greatly between the NPA and IEC results. The IEC methods consider all gross wave energy interacting with the device to be theoretically available for conversion, which ranges from 536 kWh for Miami to 3.2 million kWh for PacWave. This initial finding highlights the differences between the IEC wave resource assessment and WEC NPA methodologies and supports the need for developing novel methods that focus on power absorption.

**Table 4.** Instantaneous maximum power for all WEC sizes at all sites via NPA for 2000–2010.

Location	1 m WEC	2 m WEC	5 m WEC	10 m WEC
PacWave, OR, USA	47.8 kW	176 kW	$1.01 \times 10^3$ kW	$3.52 \times 10^3$ kW
Los Angeles, CA, USA	7.00 kW	37.1 kW	140 kW	349 kW
WETS, Oahu, HI, USA	12.2 kW	41.6 kW	236 kW	815 kW
Cape Cod, MA, USA	27.8 kW	106 kW	581 kW	$1.80 \times 10^3$ kW
Miami, FL, USA	16.4 kW	63.0 kW	329 kW	825 kW

**Table 5.** Percent reduction between the IEC gross power and net power from 2000 to 2010.

Location	1 m WEC	2 m WEC	5 m WEC	10 m WEC
PacWave, OR, USA	100%	100%	100%	100%
Los Angeles, CA, USA	83.00%	75.00%	58.70%	47.10%
WETS, Oahu, HI, USA	81.00%	68.00%	49.10%	41.10%
Cape Cod, MA, USA	82.70%	72.30%	56.10%	48.30%
Miami, FL, USA	77.90%	67.70%	56.80%	56.20%

#### 4.2.2. Monthly Power and COV

Next, the variation of power at the different study sites was examined on a monthly scale. To observe this variation, the monthly average power and monthly COV over the study period were calculated and plotted. Again, the results from the 5 m device were shown to represent these findings, as a steady progression between all WEC sizes was observed.

As indicated in Figure 17, all average net power per month is less than 150 kW for the 5 m device. In this figure, PacWave is shown to have the largest amount of net power on average throughout the year, followed by WETS, Cape Cod, Los Angeles, and Miami. This ranking of sites by absorbable power is consistent with the ranking of sites possessing the most gross power, calculated via IEC methods (see Table 3 and Figure 8). The COVs of net power for the different sites vary throughout the average year. The lowest COV for the entire year on average is found at WETS, which stays below 0.8. Cape Cod and Miami see the largest COVs throughout the year, with Miami peaking at a maximum of 5.8 in August. The larger the COV value, the more temporally unsteady the wave resource is deemed to be [22]. According to the analysis presented in Figure 17, Miami possesses the most temporally unsteady wave resource for the 5 m device. The temporally unsteady nature of August can be attributed to increased storm season activity during this month [27,29]. This site is followed by Cape Cod, which is also home to increased hurricane and tropical storm activity in the fall and winter months. Los Angeles and PacWave follow and have comparable COVs due to their spatial proximity and shared coast.

The variation of the net power at different ocean sites for all WEC sizes are studied in the following. As shown in Figure 17, the seasonal variation of the net power of WEC with varied sizes at Miami is apparent. As the WEC size increases, the magnitude of the seasonal variation increases as well. The maximum net power in the winter months ranges from 11.6 to 28 kW, while the minimum net power in summer months ranges from 2.4 to 7 kW for a 10 m device.

It is valuable to measure the efficiency of WECs of different sizes based on their Power to Volume (PV) ratios. For WETS, the site with the steadiest wave resource according to its low COV shown in Figure 17, the PV ratio is  $4.4 \times 10^5$ ,  $5.5 \times 10^4$ ,  $3.5 \times 10^3$ , and 440 kW/m<sup>3</sup> for the 1, 2, 5, and 10 m devices, respectively. This quick analysis indicates that the WECs with a smaller size generally have better efficiency than the WECs with a larger size at WETS from 2000 to 2010.

As presented in Figure 18b, the COV increases as the WEC size increases at Miami. Physically, as the WECs become larger in size, they interact with more incident wave power. In unstable wave climates such as Miami, increased interactions result in a less stable amount of proportional net power available to the larger devices (hence a larger COV for the 10 m device at this site). Unsteady wave resource is associated with increased frequency

of storms and other events that cause temporary increases or decreases in wave power. As established previously, Miami sees annual hurricane and tropical storm seasons, events that increase wave heights and subsequently wave power. These typically occur in late summer through the fall, along with the general increased storminess seen in the winter months at the location.

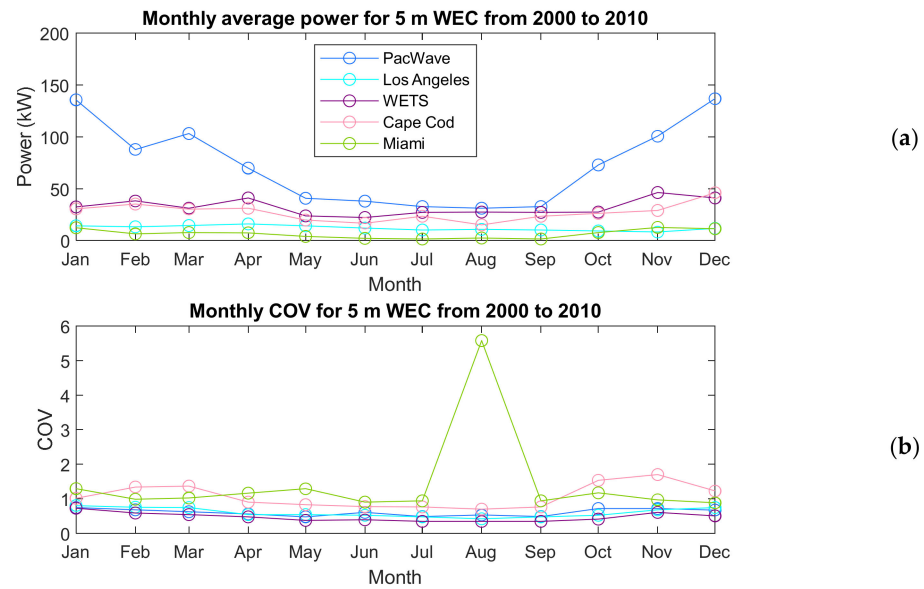


**Figure 17.** Monthly variation of (a) mean net power via NPA and (b) COV according to the baseline and expanded cases for the 5 m WEC from 2000 to 2010. Each differently colored line corresponds to one of the five ocean test sites.

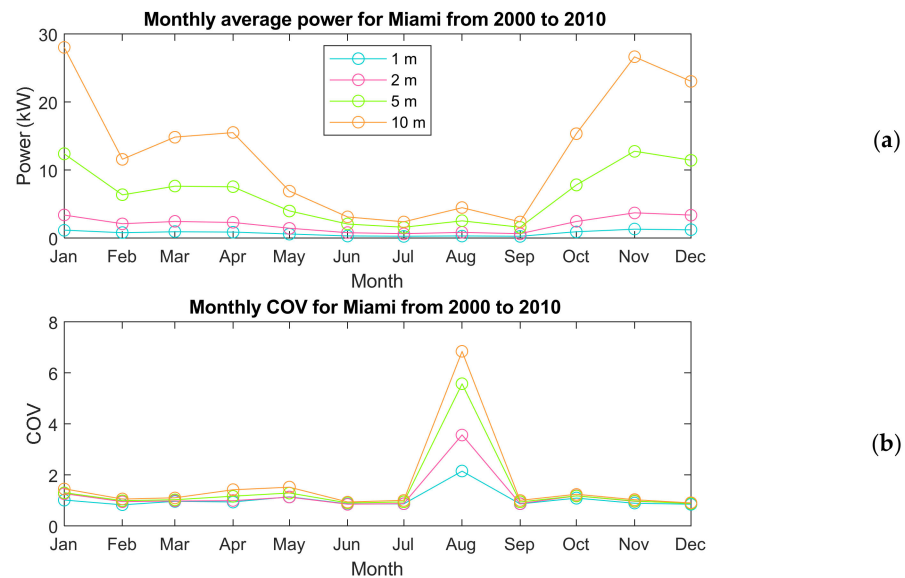


**Figure 18.** Monthly variation of (a) mean net power and (b) COV for Miami from 2000 to 2010 for all WEC sizes. Each differently colored line corresponds to one of the four test WEC sizes, described by characteristic length (i.e., body diameter) in the legend.

On the other hand, compared to Miami, WETS and Los Angeles have the most stable and wave resources of the study sites, as seen in Figures 19 and 20. Los Angeles varies the least throughout the seasons for all WEC sizes, and the COV stays below 1 for the entire year. Compared to Miami, this site offers a much more stable resource. The maximum wave power potential is 39 kW and the minimum wave power is 29.4 kW for a 10 m device. In which, the maximum available wave power assessed at Los Angeles is about 30% greater



than that assessed at Miami. This indicates not only more available power potentially at Los Angeles but also a steadier power source.

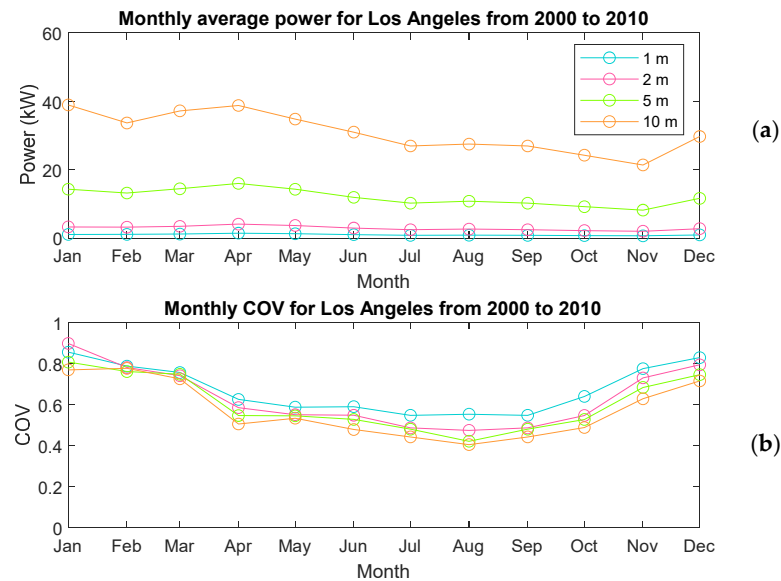


**Figure 19.** Monthly variation of (a) mean net power and (b) COV for Los Angeles from 2000 to 2010 for all WEC sizes. Each differently colored line corresponds to one of the four test WEC sizes, described by characteristic length (i.e., body diameter) in the legend.

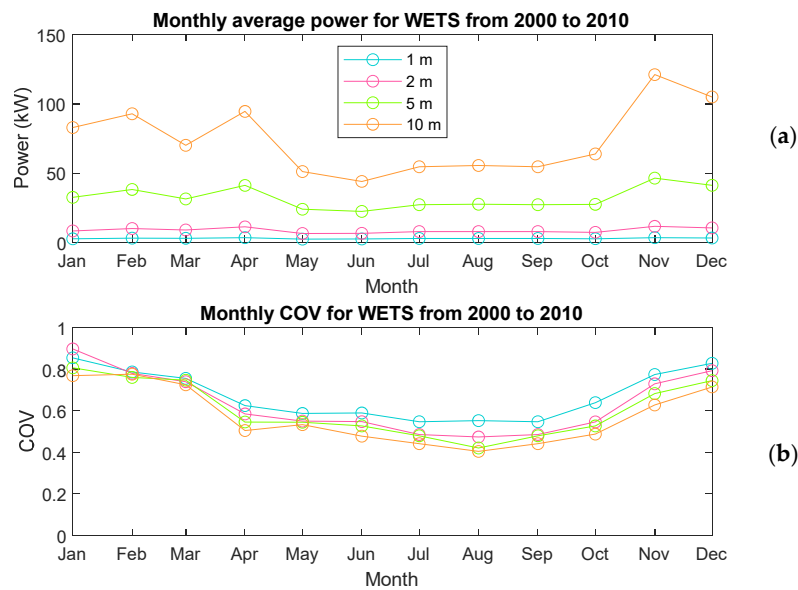


**Figure 20.** Monthly variation of (a) mean net power and (b) COV for WETS from 2000 to 2010 for all WEC sizes. Each differently colored line corresponds to one of the four test WEC sizes, described by characteristic length (i.e., body diameter) in the legend.

The steadiness of the wave source can be further reflected in the COV for Los Angeles in Figure 19b. The maximum COV of a 1 m device is 0.85 at Los Angeles, compared to the maximum COV for the 1 m device at Miami, which is 2.1. This difference is even larger for a 10 m device, which is maximum at 0.8 for Los Angeles and 6.8 at Miami. The steadier the wave resource, the lower the COV is for increasing WEC size. However, the less steady the resource, the larger the COV is for increasing WEC size.

Increased seasonal variation is visible at WETS, unlike Los Angeles. Net power increases in magnitude with device size yet continues to have a steady COV under 1 throughout the year. This can be attributed to the constant larger wave conditions seen in

the winter, compared to the outlier events that occur in Miami, which contribute to its large COV. The maximum net power of a 10 m device at WETS is 121 kW and the minimum power potential is 45 kW. The maximum net wave power is significantly larger than Miami and Los Angeles due to a greater quantity of energetic waves (as supported by Cornett [22] and Dunkle [28]).

In terms of the variation of the monthly averaged net wave power, the maximum COV of a 1 m device is 0.86, which is close to that calculated at Los Angeles.

Based on these monthly mean net power and COV assessments across WEC sizes and ocean sites, it is possible to estimate which WEC sizes would be desirable in the various locations. Generally, smaller devices encounter less variety of wave heights and periods and, therefore, could expect to be more consistent in net power absorption than a larger device, such as the 10 m WEC. If the steadiness of the net wave power is the most important criteria for a WEC designer, a 2 m device would be a better option than a 10 m WEC at Miami. However, at WETS and Los Angeles, a 10 m WEC always seems to be the best option due to the low COVs and the high values of the monthly mean net power. Therefore, steadiness of wave resource based on COV is an important metric to consider when assessing the size of the device to be deployed.

#### 4.2.3. Instantaneous Power

Resolving years' worth of wave power data to averages can understandably downplay the difference between individual net power measurements. To illustrate the results of the NPA at a higher resolution, an excerpt of the time series of net power,  $P_{net}$ , was plotted both with fixed WEC size and fixed deployment site. Additionally, the percent reductions between the IEC-calculated gross power and the net power calculated via the NPA were evaluated.

All WEC sizes had a similar progression of wave power in terms of magnitude per site, so the 1 and 10 m device results are shown to represent instantaneous power. Figure 21 shows an example of instantaneous power from January 2000 at all study sites for the 1 m WEC.

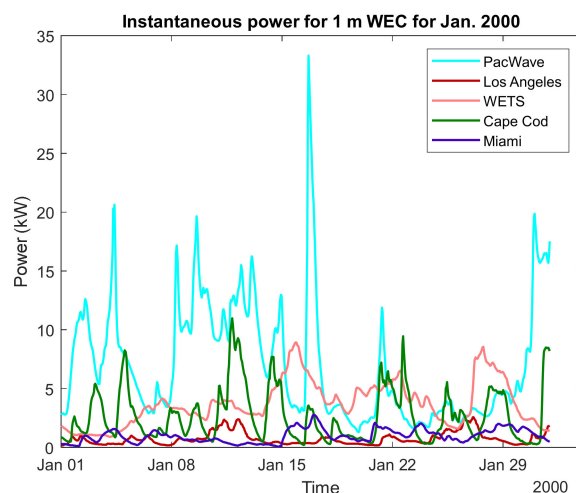


**Figure 21.** Example of instantaneous power for 1 m WEC at all sites in January 2000. Each differently colored line corresponds to one of the five ocean test sites.

As expected, PacWave possesses the most amount of wave power (averaging 7 kW) for most of the example month, while Cape Cod and WETS have the maximum value at certain times throughout January 2000. Los Angeles has the lowest amount of wave power throughout the month. In addition to the amount of the wave power potential, it is also interesting to evaluate the steadiness of the available wave power of a 1 m WEC at different locations in a higher resolution. The COV of the wave power potential across January are 0.71, 0.74, 0.5, 0.83, and 0.60 at PacWave, Los Angeles, WETS, Cape Cod, and Miami,

respectively, for the 1 m WEC. From these numbers, it is possible to conclude that the wave power potential is steadier at WETS, followed by Los Angeles, PacWave, Miami, and Cape Cod (mostly maintaining consistency with the findings in Section 4.2.2).

As WEC size increases, instantaneous power increases as well. Figure 22 shows the instantaneous power example for the 10 m WEC in January 2000. As with the 1 m device, certain times see WETS or Cape Cod possessing the maximum overall instantaneous power value, yet overall, PacWave has the most power (averaging 343 kW) recorded at most intervals. As far as the steadiness of the wave power is concerned, the COV of the power potential of a 10 m device at PacWave, Los Angeles, WETS, Cape Cod, and Miami are 0.74, 0.72, 0.58, 1.1, and 0.95, respectively. Compared to a 1 m device, it is apparent that a smaller device will have a steadier power production potential.

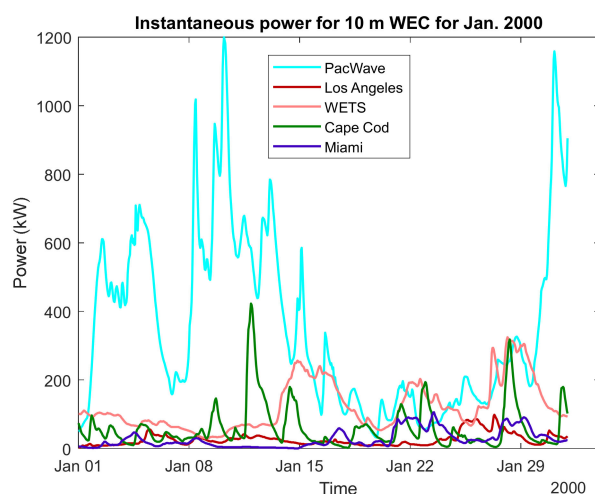


**Figure 22.** Example of instantaneous power for 10 m WEC at all sites in January 2000. Each differently colored line corresponds to one of the five ocean test sites.

A table of maximum instantaneous power recordings is presented in Table 4 for further evaluation. The maximum was taken from the entire 11 years of instantaneous power measurements. WETS, despite having greater overall MAEP (as shown in Figure 16a, 1047 kW for the 5 m WEC) and monthly average wave power than Miami (MAEP of 229 kW) and Cape Cod (MAEP of 896 kW), has lower maximum instantaneous power for all WEC sizes compared to the two sites. Again, this speaks to the steadiness of the resource at the site; relatively lower instantaneous maximum net power measurements but high average net power indicates that the wave resource at WETS is stable, and less prone to spike. Cape Cod and Miami both have fewer steady resources in comparison, and relatively high maximums for instantaneous power can be associated with conditions present during hurricanes, tropical storms, and Nor'easters.

This unsteadiness can be seen in Figure 23, where Cape Cod's instantaneous power for all WEC sizes is shown for January 2000. Here it is possible to see that all net power values spike despite WEC size at certain instances, going from close to 0 kW to values such as 340 kW, for example, for the 10 m WEC on 29 January. Increased magnitude and frequency of spikes in net power indicate a progressively fluctuating resource, an important consideration to take into account when determining WEC deployment location and optimization. The peak-to-average ratio of the wave power potential of a 1 m and a 10 m WEC are 4.2 and 7, respectively.

On the other hand, WETS has a much steadier profile of resource, as seen in Figure 24. As device size decreases, the net power measured has less variation. This was expected since the smaller devices interact with fewer incident waves. The maximums are more localized than those of Cape Cod as well. This type of behavior of net power indicates the wave resource is steadier and, therefore, more dependable. Specifically, the peak-to-average

ratio is 2.4 and 2.6 for a 1 and 10 m WEC, respectively, at WETS, which are clearly smaller than Cape Cod.

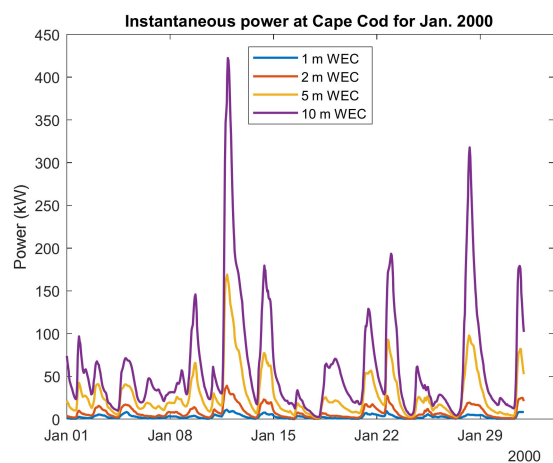


**Figure 23.** Example of instantaneous power at Cape Cod in January 2000. Each differently colored line corresponds to one of the four test WEC sizes, described by characteristic length (i.e., body diameter) in the legend.

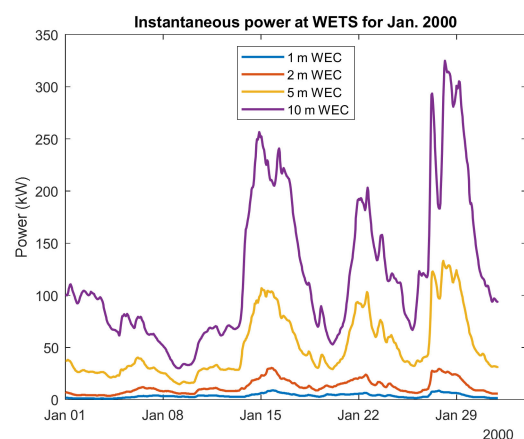


**Figure 24.** Example of instantaneous power at WETS in January 2000. Each differently colored line corresponds to one of the four test WEC sizes, described by characteristic length (i.e., body diameter) in the legend.

Table 5 shows the percent reduction between the IEC-calculated gross wave power available to the devices and the net power calculated in the NPA over the course of the study period. The percent reduction was found via Equation (12) and is a metric that allows for understanding just how great the difference is between the gross and net powers calculated for each WEC. This metric acts as a sort of quantitative efficiency measurement; the lower the percentage value, the less difference there is between the gross power and net power, meaning a greater portion of gross power is absorbed. In general, when the percent reduction is low for a specific device and location, there is an opportunity to obtain net power absorption close to the theoretical maximum net power.

Notably, PacWave has a 100% percent reduction for all WEC sizes between the gross and net power. PacWave has some of the most wave power in the world, and limiting the absorbable power through the NPA methods determined that a small fraction of gross wave power is available for absorption. The fraction of net power is so insignificant that it is not reflected in the percent reduction between the two methods for net power calculation. Across the sites, as WEC size increases, the percent reduction decreases. This was expected since larger devices can convert greater amounts of gross power. WETS has the lowest

percent reduction between the gross and net power for the larger devices, while Miami has the lowest COVs for the 1 and 2 m devices.

At the same time, it is important to note that low percent reduction per WEC size does not correlate to a low COV value. Percent reduction simply considers the entire amount of net power absorbable over 2000–2010 calculated via the IEC and NPA methods, and then compares the two. COV is a metric that describes the temporal steadiness of the resource based on statistical measurements.

## 5. Discussion

This study has thoroughly established that WEC net power assessment methods are beneficial for determining absorbable wave power for devices, instead of relying on existing IEC methodology. While NPA methods are proposed and evaluated in this work, there are certain limitations to the methods that must be discussed.

As mentioned in previous sections, the proposed NPA approach applies the radiated power limit and Budal's upper bound, which both have drawbacks. For example, the radiated power limit always assumes an optimal oscillation without taking the actual dimensions of the device into consideration. In this vein, this theoretical power limit is highly unpractical when the incident waves are very energetic (e.g., the device may be out of water or fully submerged in the water, but it is still assumed to be interacting with ocean waves).

As far as Budal's upper bound is concerned, it becomes unrealistic when the ocean wave has a high frequency (low period). Since, theoretically, Budal's upper bound always assumes the body volume is fully utilized, the limit is not applicable when the wave becomes less energetic. Therefore, the current values of net power found for the devices may be thought of as the absolute maximum net power absorbable (theoretically), which will be considerably larger than the actual wave power production in practice. In summary, the proposed NPA methods output the ideal, absolute maximum amount of power a device may absorb, agnostic of WEC size.

Moreover, this study was completed for a basic, heaving spherical WEC and provides a meaningful wave power potential assessment technique and analysis for WEC developers. As mentioned in previous sections, there is a clear need for developing a WEC NPA technique to evaluate the wave power potential for generic WECs (across sizes, degrees of freedom, shapes, etc.). Therefore, this study can be further extended to encompass this variation; there is current research attempting to mathematically extend the radiation power limit and Budal's limit to be generally applicable to arbitrary WEC archetypes. Furthermore, in the future, this study should be integrated into existing models for calculating absorbable wave power, such as the Wave-to-Wire model [28] or capacity factor analysis [30].

More work is also required to further study the relationship between the gross power, the radiation power limit, and Budal's upper bound. Although the absorbable wave power can never theoretically exceed the available power in the wave (gross power), it was consistently found in this study that a significant portion of the radiation power limit (especially for large periods) and Budal's upper bound (especially for low periods) are larger than the gross power, which physically cannot occur. As discussed in this section, there are certain theoretical limitations of the radiation limit and Budal's upper bound, which may be one driver of this phenomenon.

At the same time, the accuracy of the calculation of gross power is also unclear. In current theory, only the characteristic area of a device must be considered to compute the gross power. For example, a tall WEC (height = 100 m) and a short WEC (height = 0.1 m) will have identical gross power if they have the same waterplane cross-sectional area, which is unrealistic. Additionally, the shape of the device is not taken into consideration when calculating gross wave power, meaning a cylindrical-shape device and a box-shape device will have the same gross power if they have the identical free surface cross-sectional area.

One convincing way to validate and provide more insight and deeper understanding of this research is to conduct experimental tests and compare with the real behavior of

WECs (with the implementation of a PTO unit). There must be increased testing of WECs in wave tanks and ocean conditions corresponding to the typical sea states observed in deployment locations. Valuable future studies may include physical validation for the modeled wave data scenario presented in this study. Temporal and spatial availability of wave power will also vary depending on additional environmental factors, such as ocean currents and wind, along with other forces depending on location. Validating this study with real wave observation data would only strengthen (or disprove) the case for utilizing NPA methods for evaluating absorbable WEC power.

## 6. Conclusions

Conventional IEC techniques for wave resource assessments evaluate the wave power potential purely dependent on general wave characteristics, which was expected to significantly overestimate the net power since a considerable portion of the wave power is not absorbable. Therefore, this assessment was conducted directly from a WEC device point of view. However, there exists a large variety of WEC archetypes in development and literature. Accordingly, there is a clear need for developing a new wave power assessment technique directly from a device point of view, which is generally applicable across WEC archetypes.

Therefore, a novel WEC net power assessment technique was proposed and developed in this research by implementing the radiation power limit and Budal's upper bound, both used for arbitrary heaving axisymmetric devices. In addition to the contribution of the theoretical developments, the developed new technique is also applied to evaluate the potential wave power of WECs with different sizes (1, 2, 5, and 10 m) at various ocean sites (PacWave, Oregon; WETS, Hawaii; Cape Cod, Massachusetts; Los Angeles, California; Miami, Florida) by using modeled wave data to provide meaningful insights for WEC developers.

The simulation results show the wave power potential predicted by the proposed NPA methodology is significantly lower than the power predicted by the conventional IEC technique (the annual mean power reduced by 99.2 % at PacWave for a 5 m WEC). Specifically, the deployment sites of Los Angeles, California and Miami, Florida are dismissed in the wave energy conversion field because of their uncapturable fraction of resources compared to more energetic sites by using the IEC method. However, this study showed that these two ocean sites have considerable amounts of wave energy (396 and 229 kW, respectively, compared to 2444 kW at PacWave for a 5 m WEC) by utilizing the proposed NPA technique. This study also shows that PacWave has the most energetic wave resource (for a 5 m device the maximum monthly average power is 137 kW) and WETS has the steadiest potential wave power (average monthly COV of 0.6 for the 5 m WEC). The monthly average power analysis further indicates that a larger device (e.g., 10 m) has potentially better performance regarding the amount and steadiness of wave power production at WETS and Los Angeles compared to a small device. Finally, the available wave power of WECs with different sizes at different ocean sites was further analyzed at a higher resolution (every 3 h). The maximum instantaneous power at PacWave for the 1 and 10 m devices was found to be 33.3 and  $1.2 \times 10^3$  kW, respectively.

In the future, it is essential to further study the relationship between the radiation power limit, Budal's upper bound, and gross wave power (particularly with regard to the reasoning why theoretical upper bounds can exceed the gross wave power). Additionally, this study needs to be further extended to a more generic WEC NPA method that is generally applicable to WECs with arbitrary degrees of freedom, shapes, and sizes.

**Author Contributions:** G.D. collected and analyzed the study data and wrote the initial draft papers and final paper. S.Z. aided in data interpretation and provided major revisions of the initial draft papers. B.R. conceived the concept for the study, aided in data interpretation, and provided major revisions of the initial draft papers. All authors have read and agreed to the published version of the manuscript.

**Funding:** This research received no external funding.

**Data Availability Statement:** Wu, W., Wang, T., Yang, Z., García-Medina, G. Development and validation of a high-resolution regional wave hindcast model for U.S. West Coast wave resource characterization. Available upon request. <https://doi.org/10.1016/j.renene.2020.01.077>. Allahdadi, M., Gunawan, B., Lai, J., He, R., Neary, V. Development and validation of a regional-scale high-resolution unstructured model for wave energy resource characterization along the US East Coast. <https://doi.org/10.1016/j.renene.2019.01.2020>.

**Conflicts of Interest:** The authors declare no conflict of interest. The funders had no role in the design of the study; in the collection, analyses, or interpretation of data; in the writing of the manuscript, or in the decision to publish the results.

## References

1. Columbia Power Technologies. Why Wave Energy? 2019. Available online: <https://cpower.co/why-wave-energy/> (accessed on 20 November 2021).
2. Hashemi, M.R.; Neill, S.P. *Fundamentals of Ocean Renewable Energy*, 1st ed.; Academic Press, Ed.; Elsevier: Amsterdam, The Netherlands, 2018.
3. LiVecchi, A.; Copping, A.; Jenne, D.; Gorton, A.; Preus, R.; Robichaud, R.; Green, R.; Geerlofs, S.; Gore, S.; Hume, D.; et al. *Powering the Blue Economy: Exploring Opportunities for Marine Renewable Energy in Maritime Markets*; U.S. Department of Energy, Office of Energy Efficiency and Renewable Energy: Washington, DC, USA, 2019.
4. Driscoll, B.P.; Gish, L.A.; Coe, R.G. A Scoping Study to Determine the Location-Specific WEC Threshold Size for Wave-Powered AUV Recharging. *IEEE J. Ocean. Eng.* **2020**, *46*, 1–10. [[CrossRef](#)]
5. Jin, S.; Zheng, S.; Greaves, D. On the scalability of wave energy converters. *Ocean Eng.* **2022**, *243*, 110212. [[CrossRef](#)]
6. Dunkle, G.; Robertson, B.; Garcia-Medina, G.; Yang, Z. PacWave Wave Resource Assessment. 2020. Available online: [https://ir.library.oregonstate.edu/concern/technical\\_reports/hm50tz68v](https://ir.library.oregonstate.edu/concern/technical_reports/hm50tz68v) (accessed on 23 September 2021).
7. Todalshaug, J.H. Hydrodynamics of WECs. In *Handbook of Ocean Wave Energy*; Pecher, A., Kofoed, J.P., Eds.; Springer International Publishing: Cham, Switzerland, 2017; pp. 139–158.
8. Budal, K.; Falnes, J. Interacting Point Absorbers with Controlled Motion. In *Power from Sea Waves*; Count, B.M., Ed.; Academic Press: London, UK, 1980; pp. 381–399.
9. Newman, J.N. *Marine Hydrodynamics*, 40th Anniversary ed.; The MIT Press: London, UK, 2018.
10. Budal, K.; Falnes, J. Wave power conversion by point absorbers: A Norwegian project. *Int. J. Ambient Energy* **1982**, *3*, 59–67. [[CrossRef](#)]
11. Falnes, J. A review of wave-energy extraction. *Mar. Struct.* **2007**, *20*, 185–201. [[CrossRef](#)]
12. Falnes, J. Oscillating-Body Wave-Energy Converters. In *Ocean Waves and Oscillating Systems: Linear Interactions Including Wave-Energy Extraction*; Falnes, J., Kurniawan, A., Eds.; Cambridge University Press: New York, NY, USA, 2020; pp. 204–241.
13. Falnes, J. Small is Beautiful: How to Make Wave Energy Economic. *Proc. EBC Congr.* **2003**, *29*, 481–489.
14. Todalshaug, J.H. Practical limits to the power that can be captured from ocean waves by oscillating bodies. *Int. J. Mar. Energy* **2013**, *3–4*, e70–e81. [[CrossRef](#)]
15. Beatty, S.J.; Hall, M.; Buckham, B.J.; Wild, P.; Bocking, B. Experimental and numerical comparisons of self-reacting point absorber wave energy converters in regular waves. *Ocean Eng.* **2015**, *104*, 370–386. [[CrossRef](#)]
16. IEC TS 62600-101:2015; Marine Energy–Wave, Tidal and Other Water Current Converters–Part 101: Wave Energy Resource Assessment and Characterization. International Electrotechnical Commission: Geneva, Switzerland, 2015.
17. Evans, D.V. A theory for wave-power absorption by oscillating bodies. *J. Fluid Mech.* **1976**, *77*, 1–25. [[CrossRef](#)]
18. Holthuijsen, L.H. *Waves in Oceanic and Coastal Waters*; Cambridge University Press: New York, NY, USA, 2007.
19. Falnes, J.; Hals, J. Heaving buoys, point absorbers and arrays. *Philos. Trans. R. Soc. A Math. Phys. Eng. Sci.* **2012**, *370*, 246–277. [[CrossRef](#)] [[PubMed](#)]
20. Hals, J.; Falnes, J.; Moan, T. Constrained optimal control of a heaving buoy wave-energy converter. *J. Offshore Mech. Arct. Eng.* **2010**, *133*, 011401. [[CrossRef](#)]
21. Tethys Engineering. RM3: *Wave Point Absorber*; U.S. Department of Energy: Washington, DC, USA, 2021.
22. Cornett, A.M. A global wave energy resource assessment. In Proceedings of the Eighteenth International Offshore and Polar Conference, Vancouver, BC, Canada, 6–11 July 2008; Volume 50.
23. Stopa, J.E.; Cheung, K.F.; Chen, Y.L. Assessment of wave energy resources in Hawaii. *Renew. Energy* **2011**, *36*, 554–567. [[CrossRef](#)]
24. Kilcher, L.; Thresher, R. *Marine Hydrokinetic Energy Site Identification and Ranking Methodology Part I: Wave Energy*; National Renewable Energy Laboratory: Golden, CO, USA, 2016.
25. Wu, W.C.; Wang, T.; Yang, Z.; García-Medina, G. Development and validation of a high-resolution regional wave hindcast model for U.S. West Coast wave resource characterization. *Renew. Energy* **2020**, *152*, 736–753. [[CrossRef](#)]
26. Allahdadi, M.N.; Gunawan, B.; Lai, J.; He, R.; Neary, V.S. Development and validation of a regional-scale high-resolution unstructured model for wave energy resource characterization along the US East Coast. *Renew. Energy* **2019**, *136*, 500–511. [[CrossRef](#)]

27. Dolan, R.; Davis, R.E. Coastal Storm Hazards. *J. Coast. Res.* **1994**, *12*, 103–114.
28. Dunkle, G. Wave Resource Assessments: Spacio-Temporal Effect of Wave Energy Converter Scale and Blue Economy Opportunities. Master's Thesis, Oregon State University, Corvallis, OR, USA, 2021.
29. Brown, D.P.; Beven, J.L.; Franklin, J.L.; Blake, E.S. Atlantic hurricane season of 2008. *Mon. Weather Rev.* **2010**, *138*, 1975–2001. [[CrossRef](#)]
30. Babarit, A.; Hals, J.; Muliawan, M.J.; Kurniawan, A.; Moan, T.; Krokstad, J. Numerical benchmarking study of a selection of wave energy converters. *Renew. Energy* **2012**, *41*, 44–63. [[CrossRef](#)]